Express Polymer Letters Vol.17, No.5 (2023) 546–562
Available online at www.expresspolymlett.com
https://doi.org/10.3144/expresspolymlett.2023.40

Research article

Molecular dynamics on blend miscibility of LLDPE and soft wax: An atomistic simulation and thermodynamic approach

Mafereka Francis Tyson Mosoabisane[1], *Cornelia Gertina Catharina Elizabeth Van Sittert*[2], *Adriaan Stephanus Luyt*[3*]

[1]Department of Chemistry, University of the Free State (Qwaqwa Campus), Phuthaditjhaba, South Africa
[2]Laboratory of Applied Molecular Modelling, Research Focus Area of Chemical Resource Beneficiation, North-West University, Potchefstroom, South Africa
[3]Center for Advanced Materials, Qatar University, Doha, Qatar

Received 8 September 2022; accepted in revised form 28 December 2022

Abstract. Atomistic molecular dynamics and dissipative particle dynamics simulations have been applied to study the miscibility of long- and short-chain linear low-density polyethylene (LLDPE)/wax blends. Molecular dynamics (MD) studies focused on selected mass ratios of LLDPE/wax blends to compare the simulations to published experimental results. The solubility parameters of the pure components and blends were computed to determine the Flory-Huggins interaction parameter (χ_{AB}) of the binary systems. Because the critical Flory-Huggins interaction parameter $(\chi_{AB})_{critical}$ was larger than χ_{AB} for all the mass ratios investigated, wax and LLDPE were expected to be completely miscible at all mass ratios. The results from the Flory-Huggins interaction parameter agree with the modelled glass transition temperature (T_g) values obtained for the blends. However, these results could not be used to explain the blends' miscibility characteristics because the highly crystalline wax does not show a glass transition. The partial miscibility of the blends was, however, observable from the dissipative particle dynamics (DPD) simulation results. These results showed clumps of wax chains in the blend matrices. The simulation results further showed that the wax chains interacted more strongly with the short than with the long LLDPE chains, which was the final observation that supported the partial miscibility of the wax and LLDPE in the LLDPE/wax blends.

Keywords: *modeling and simulation, miscibility, LLDPE, wax, thermodynamics*

1. Introduction

Polyethylenes contribute significantly to the production of commodity plastic materials because of their wide variety of properties. These properties include low dielectric constant, low cost, and ease of processing [1] due to the variation of parameters such as molecular weight, branching, and molecular weight distribution [2].

Linear low-density polyethylene (LLDPE) is a polyethylene formed by the copolymerization of ethylene and α-olefins such as 1-butene, 1-hexene, and 1-octene [3]. The production of LLDPE is usually done at low pressures and temperatures, which means less energy and cheaper production costs. The physical blending of wax (which is non-toxic and cheap) with LLDPE offers even better material due to its softening and plasticising effects. Physically blended LLDPE/wax blends are therefore better for heat transportation and thermal energy storage than pure LLDPE.

Phase change materials (PCMs) are substances that release or absorb a large amount of energy in the form of latent heat during melting or solidification [4]. Wax with a range of phase change temperatures can store thermal energy as latent heat [5, 6]. It has a high heat of fusion and can resist chemicals, and therefore

---

[*]Corresponding author, e-mail: riaanluyt2@gmail.com

it is a good PCM [1, 7, 8]. Blends created from wax and polyethylenes, particularly LLDPE, are highly preferred as PCMs. One possible application of the LLDPE/wax blends is their use as a temperature buffer in the energy conservation of buildings [3, 5]. The miscibility of the blends is influenced by the type of polyethylene matrix and the type of wax, as well as the wax content [9, 10].

The blends' miscibility determines the phase morphology and the properties. The first step in predicting the properties of polymer blends is to understand polymer miscibility/compatibility [11]. It is imperative to study miscibility relative to the interaction of pure components in a blended system because it provides clear direction in designing the materials for specific usage. Polymer blends are classified as miscible, immiscible, and compatible [12].

Besides the great benefits acquired through blending, polymer blend miscibility poses many peculiar problems of research interest. Although much experimental work covering the thermal and mechanical properties possessed by different polyethylene/wax blends has been done, little or almost no success has been achieved in establishing the exact morphology responsible for these properties [13, 14].

The study of the miscibility of LLDPE blended with other polyethylenes has been reported using various research methods [15, 16]. Most research reporting on miscibility is experimental rather than computational, such as molecular dynamics (MD) [15–17]. One particular study done with molecular dynamics simulations investigated the influence of branch content on the miscibility of high-density polyethylene (HDPE)/butane-LLDPE blends. This study investigated the effect of branch content [18], and it showed that 40 branches or more per 1000 carbons are required for phase separation of blends to occur in the melt regardless of temperature. Another study using molecular dynamics investigated the influence of chain length during the heating and cooling process by reporting on the polyethylenes' molecular structure and properties [19]. The bond orientation parameter (the standard measure of order used in polymer systems) values for short-chain polymers were larger than those of the long-chain polymers after freezing because chains in the crystalline fractions of polymers are generally folded. The modelled results were in good agreement with the experiments, which means that their MD studies were reliable. However, the interaction of wax (also short-chain polyethylenes) with LLDPE at the molecular level has not yet been investigated by computational studies to determine miscibility.

Generally, atomistic MD has been applied to study the miscibility of different types of polymer blends based on their structure and molecular weights [20, 21]. These studies investigated mostly homopolymers, such as polylactide, polyhydroxybutyrate, poly(*p*-dioxanone), and poly(vinyl phenol). However, the structures of these homopolymers are different from the structure of LLDPE with a morphology and properties that are branch content dependent. According to the Flory-Huggins theory, certain polymer blends with similar structures are miscible at all compositions based on molecular interactions [20–23]. The same theory was successfully used to predict the immiscibility of some of the polymer blends [24–26], while the miscibility of other blends depended on the composition of the components and the system's temperature. The solubility parameters of HDPE and LLDPE were computed to determine the blends' Flory-Huggins interaction parameters (χ) [18]. The calculated χ between the HDPE and LLDPE models showed irregular dependence on temperature. For an increase in branch content of the LLDPE, the computed solubility values decreased with increasing temperature.

The most common way to determine blend miscibility through molecular dynamics is to investigate the glass transition temperature of the blends [27]. One glass transition temperature is related to one continuous phase of the blend, while two transitions are related to the immiscibility of the blend components. Lodge and McLeish [28] argued that two transitions are sometimes observed due to an increase in the local concentration of monomers in the models created by the chain connectivity of the polymers. Therefore, two transition temperatures could still be observed in single-phase blend systems. It is difficult to rely on glass transition temperature as a criterion to judge immiscibility or partial-miscibility [21].

Another approach to investigate the miscibility of polymer blends is the use of dissipative particle dynamics (DPD) at the mesoscopic level. These mesoscopic dynamics studies have successfully related atomistic simulation of the blends through the Flory-Huggins theory [22, 29], whereby molecular dynamics first determine the interaction parameters before it is applied in mesoscopic dynamics simulations. These studies' outcomes have also been complemented by various experimental investigations within accepted methodology error and different capabilities of software packages [23, 30–33]. Computational chemistry helps avoid expensive trial-and-error experiments in creating polymer blends to make new materials with specific properties.

Recently published computational studies focused on specifically paraffin wax-based composites [34, 35], as well as various properties of blends and composites created from different polyethylenes and other components [36, 37]. One study looked at the polydispersity and branching effects of paraffin wax on thermal conductivity [34], while another critically compared different force fields available on the CROMACS software package, especially on a theoretical description of the n-alkane matrix [35]. MD simulations were used to investigate diffusion rates of oxygen through the polyethylene and plant-based wax (nonacosan-10-ol) blend by the Materials Science Suite of the Schrödinger software [38]. The mechanical properties and diffusion rate coefficient of oxygen in the proposed polyethylene/wax blend were improved and the new proposed material was recommended for storage of perishable products.

This study reports on the first MD simulations on the miscibility of the LLDPE/wax blends using Materials Studio software [33]. It focuses on studying the miscibility of LLDPE and wax, based on the Flory-Huggins theory. This theory focuses on the interaction and solubility parameters of the blends and pure components. The glass transition temperatures of the blends were also used to investigate the miscibility of wax with LLDPE through the cooling method. The physical properties of the blends' modelled systems were also examined in MD simulations by looking at inter and intra-chain pair correlation functions. Lastly, the miscibility of the LLDPE/wax blends was investigated through DPD simulations.

2. Experimental

2.1. Simulation method

Materials Studio (MS) molecular modelling software (Accelrys Inc.) [33] through the Centre for High Performance Computing (CHPC), situated on the Rosebank campus at the University of Cape Town in South Africa, was used to do the modelling calculations. The simulations were done through a main system at the CHPC, which uses a supercomputer cluster called Lengau (1368 compute nodes, 5 large memory nodes, 9 GPU nodes, 4 PF storage over the Lustre parallel file system) of the Council for Scientific and Industrial Research (CSIR). A personal computer (Dell OptiPlex 9020, 2xQuad core Intel i7-4770s 3.10 GHz, 16 GB RAM, 1TR GB HDD), situated at the University of the Free State (Qwaqwa Campus), was utilized as the workstation.

2.2. Construction of monomer models

The two monomers, ethylene and 1-hexene were drawn manually in the visualization module of Materials Studio software [33]. These two monomers were used as starting compounds for the synthetic catalytic polymerization of LLDPE under specific pressure and temperature conditions.

2.3. Optimisation of monomers with DFT

The two monomers, ethylene, and α-olefin (1-hexene), were constructed and geometrically optimised using the density functional theory module (DFT-DMol^3) in the Materials Studio software [33, 39]. The generalized gradient approximation function of Perdew and Wang (GGA-PW91) was used [40, 41] with a double numeric polarised basis set with an additional diffuse function (DNP+). The DNP+ basis set was chosen because it was tested satisfactorily against polymers and surfaces [42], especially for calculations that require a very large orbital cut-off [40]. Geometry optimisation was done at convergence tolerance as follows: quality (medium), energy ($2.0\cdot10^{-5}$ kcal·mol^{-1}), maximum force (0.004), maximum iterations (50), maximum time step (0.3 fs) and 0.005 Å displacement, no symmetry, unrestricted spin state, triplet multiplicity, and zero charges. The electronic setup was as follows: integration accuracy (medium), self-consistent-field (SCF) settings at medium (with tolerance $1.0\cdot10^{-5}$, maximum of 50 SCF cycles, multipolar expansion hexadecapole, with a global orbital cut-off scheme and smearing of 0.005), all electron core treatment, and medium orbital cut-off quality.

2.4. Construction and optimisation of LLDPE with a forcefield

Optimised ethylene and 1-hexene structures were used to construct many single LLDPE polymer chains with chain lengths from 10 to 500 (20 to 1000 backbone carbons) with branches of different 1-hexene content randomly distributed along the backbone using forced concentrations [43]. The random copolymer interface, which is found in the build polymers of the MS software [33], was used to create the

LLDPE chains. However, the polymerize option within a random copolymer interface made it possible to first insert the two constructed monomers into two separate columns of the template. The polymerize tab has many other options, such as using forced concentrations or reactivity ratios (which allows variation of branches along the polymer backbone) and chain length and/or the number of chains that determine the size and shape of the polymer molecule. The constructed single LLDPE polymer chains were further minimized geometrically using the force field called condensed-phase optimised molecular potentials for atomistic simulation studies (COMPASS) [44]. COMPASS is an ab initio force field that is consistently parameterised for big molecules such as polymers in a condensed state. Geometry optimisation was done with the quasi-Newton algorithm because it converged and minimized the LLDPE structures faster than other algorithms. The convergence tolerance setup was as follows: quality (customized), energy ($2.0\cdot10^{-5}$ kcal·mol^{-1}), maximum force ($2.0\cdot10^{-5}$ kcal·mol^{-1}·Å^{-1}), different maximum iterations, and 0.005 Å displacement. The contribution of charges to the minimized energy was calculated with the original Gasteiger method within a maximum of 50 iterations for a convergence limit of $2.0\cdot10^{-5}$.

2.5. Construction and optimisation of wax

The ethylene monomer from the database of MS was used to construct the wax chains. The constructed wax chains with different lengths ($C_{20}H_{22}$–$C_{44}H_{46}$) were geometrically optimised using the Forcite module with the COMPASS force field [44]. Geometry optimisation was done with the quasi-Newton algorithm because the energy convergence is fast and good for short-chain polyethylenes. Periodic wax models, needed for MD simulations were created using the Amorphous Cell module in MS. The periodic systems were relaxed with the canonical constant number, volume, and temperature (NVT) ensemble MD simulation, followed by an isothermal–isobaric (constant number, pressure, and temperature) (NPT) ensemble MD simulation at 298 K for 2000 ps and a 0.1 fs time step.

2.6. Building three-dimensional periodic systems of LLDPE/wax blends

Cubic simulation boxes, often called periodic systems, were created with the Amorphous Cell module in Materials Studio. Both the LLDPE and wax models were added to the periodic cells to create blend systems of different weight ratios through the technique described by Theodorou and Suter [45]. The Amorphous Cell calculation module was chosen over the construction (legacy) module because it is convenient to vary the number of chains per box. Additionally, the construction process is shorter than using the construction legacy. The setup was as follows: cubic construction type of lattice, the initial density of 0.924 g·cm^{-3} for LLDPE and 0.900 g·cm^{-3} for wax. Torsion angles were calculated during construction while optimising the chains but not the cells. A quasi-Newton algorithm was used to a convergence energy level of 0.00002 kcal·mol^{-1} for smaller molecules and 0.001 kcal·mol^{-1} for large molecules. The energy setup for the cells was as follows: COMPASS was chosen as the force field, charges were calculated by the Gasteiger (Gast_original1.0) method, Ewald summation was used as the electrostatic summation method, while atom-based calculations were used for the van der Waals forces.

2.7. Molecular dynamics (MD) details

Molecules of the LLDPE chains (70 branches per 520 carbons in the backbone) and wax chains with 36 carbons long were added to the periodic systems. In order to compare the models with the experimental results, the blend systems had composition ratios as follows: 95/5, 90/10, 80/20, 70/30, and 60/40 w/w LLDPE/wax. The chains in the periodic systems were relaxed by first using the NVT ensemble, followed by NPT MD to further equilibrate the chains. A similar process was followed using a unit cell containing short chains of LLDPE (1 branch per 100 carbons in the backbone) and wax (36 carbons) molecules to investigate the short LLDPE chains' effect on miscibility with wax. All MD simulation studies were run in the bulk state, meaning without a solvent.

The LLDPE and wax chains in the periodic system were further relaxed by annealing from 150 to 450 K and back to 150 K with a heating ramp of 0.1 K·ps^{-1} for 30 cycles, first with NVT followed by NPT MD [32] for $1.0\cdot10^{5}$ steps and a 1.0 fs time step. Torsion angles were calculated automatically at 0.25 radii of van der Waals energy and loading steps of 1000 ps and 0.1 fs. The partial charge of the atoms was estimated using the charge equilibration method. Electrostatic energy was calculated by the Ewald summation method at an accuracy level of 0.0001 kcal·mol^{-1} (fine). The atom-based summation was adopted for van der Waals interaction with a cut-off distance of 15.5 Å. After the 30 cycle annealing, a 1000 ps NVT MD simulation was carried out for $1.0\cdot10^5$ steps and 1.0 fs step time, followed by NPT MD for 1000 ps total simulation time at 298 and 500 K, with the same steps and step time. A random initial velocity was applied in all the simulations, and a 0.01 q ratio using a Nosé-Hoover-Langevin (NHL) [46] algorithm and Berendsen barostat to keep the volume or pressure constant.

Molecular dynamics was repeated with the NPT ensemble at different temperatures starting from 500 to 100 K at 1000 ps without changing the settings. After all the MD runs for all the molecules were completed, the blends' relaxation or glass transition temperatures (T_g) were determined from the plots of thermal expansion versus temperature. Thermal expansion versus temperature data was further used to study the miscibility of the various blends.

The Hildebrand solubility parameters (δ) of the neat LLDPE, neat wax, and the blends were calculated by cohesive energy density (CED), built into the Forcite module. The obtained solubility values were then used to compute the interaction parameters of LLDPE/wax blends of different weight ratios at 298 and 450 K. The calculated interaction parameters of the blends were compared to their critical interaction parameters for the prediction of miscibility between the blend components. The radial distribution functions of the blends were plotted against temperature to determine the interaction between LLDPE and wax chains in terms of interatomic and intra-atomic interactions.

2.8. Dissipative particle dynamics (DPD) simulation of LLDPE/wax blends

One of the advantages of simulating polymer blends with mesoscopic dynamics and dissipative particle dynamics (DPD) is that results are generated faster than with atomistic simulations or experiments. In mesoscale dynamics, it is common practice to group atoms together in the form of beads. This approach reduces the simulation time compared to the atomistic simulations. Therefore, less CPU time is required to run the calculations, and big systems can be simulated. The correlation between atomistic simulations and mesoscopic dynamics can be investigated by comparing the repulsive and Flory-Huggins interaction parameters obtained by applying the Flory-Huggins theory.

When doing DPD simulations, a group of atoms is represented by a bead. The different beads interact with each other instead of with small atoms, considerably reducing the simulation time. The interacting beads must obey Newton's equation of motion (Equation (1)) [47]:

$$\frac{\mathrm{d}r_i}{\mathrm{d}t} = v_i;\ \frac{\mathrm{d}v_i}{\mathrm{d}t} = f_i \tag{1}$$

where r_i and v_i are the position and velocity of the i^{th} particle in the simulation, and t is time. The masses of the beads are normalized to 1, and the total force f_i acting on a specific particle is a combination of three pairwise contributions: a conservative force F^C, a dissipative force F^D, and a random force F^R (Equation (2)):

$$f_i = \sum_{j\neq i}\left(F_{ij}^{C} + F_{ij}^{D} + F_{ij}^{R}\right) \tag{2}$$

The sum runs over all the particles within a chosen cut-off radius r_c.

The interactions of the DPD beads are mapped onto the Flory-Huggins theory through the interaction parameter (χ). If the system has beads interacting with each other, assuming that they are equal, then $a_{ii} = a_{jj}$, and their total density ($a_{ii} + a_{jj}$) are constant throughout. According to Groot and Warren [47], the mapping relation from atomistic simulations to DPD is formulated in Equation (3):

$$\chi = \frac{2\alpha\left(a_{ij} - a_{ii}\right)\left(\rho_i - \rho_j\right)}{k_B T} \tag{3}$$

where the density of the system is determined by $\rho_i + \rho_j = \rho$, α is related to the pair correlation function $g(r)$ through a reduced co-ordinate $r = \mathbf{r}/r_c$. The linear relation between Flory-Huggins χ parameters and the conservative interaction strength for polymers is defined in Equation (4):

$$\alpha_{ij} = \alpha_{ii} + 3.27\chi_{ij}, (\rho = 3), \alpha_{ii} = 25 \tag{4}$$

The repulsion energy parameter between the same pair alike (α_{ii}) atoms is taken as 25. The value called the self-repulsion of beads was chosen by Groot and Warren such that a pure DPD fluid has a compressibility similar to that of liquid water. However, the interaction parameter between wax and LLDPE was determined from the solubility parameter values using Equation (5). The Flory-Huggins parameter (χ) can be mapped to the repulsive interaction parameter in DPD (Table 2).

$$\chi = \frac{V(\delta_\mathrm{w} - \delta_\mathrm{LL})^2}{RT} \tag{5}$$

where V is the molar volume of the smallest repeat unit ethylene, since both wax and LLDPE contain ethylene units [28], δ_w and δ_LL represent the solubility parameters of wax and LLDPE, respectively, R is the gas constant and T the temperature. The number of beads in each mesoscale molecule was determined by the degree of polymerisation and the characteristic ratio (C_n) of the polymer. The characteristic ratio, C_n, is the ratio of the observed end-to-end distance and the end-to-end distance of a freely jointed chain composed of n bonds of the step length of the polymer chain. Using the molar mass of the monomer (M_m) and the polymer molecular weight (M_p), n is the number of repeat units or monomers, and the number of beads in the polymer can be calculated with Equation (6):

$$n_\mathrm{DPD} = \frac{M_\mathrm{p}}{M_\mathrm{m} C_\mathrm{n}} \tag{6}$$

The solubility parameters of the pure components, namely wax, and LLDPE, were calculated using the Synthia module in Materials Studio software [33]. The molar volume of ethylene, which makes the main chain of LLDPE and wax, was also calculated in Synthia and used to determine the Flory-Huggins interaction parameter. However, the repulsion parameters used in the formulation of the DPD calculations were obtained from the Groot and Warren equation by using the calculated Flory-Huggins interaction between wax and LLDPE.

The DPD simulations of the LLDPE/wax blends were performed in a unit cell (10.7×10.7×10.7 Å) with a bead density of $\rho = 3$. The time step was set to 0.05 fs, and the nearby beads in the polymer chain interacted via a linear spring with a harmonic constant of 4.0 Hz, and the friction coefficient, γ, was chosen as 4.5. Initially, the total number of steps applied to the molecules was 1000, and when the jobs finished successfully, the total simulation time was increased to 50 000 steps for a time step of 498.45 fs. The reduced units were as follows: length of 10.7 Å, mass of 215.5 amu, and energy of 0.59219 kcal·mol^{-1}. Reduced units are special to DPD. The unit of length is normally taken as the interaction cut-off radius, r_c, the unit of mass as one bead, and the unit of energy as $k_\mathrm{B}T$ at a suitable reference temperature (usually 298 K). A dissipation radius of 1 was used, and the initial velocities were set to random. Therefore, a total of $2\cdot10^5$ DPD steps were carried out in this work. For each blend, 1000 frames were produced. The trajectories of all the blends were analysed.

3. Results and discussion

This section details the results obtained from LLDPE/wax blend systems simulations. In-depth analysis and discussions on the miscibility of the binary blend systems created from wax and LLDPE are outlined. The miscibility of blends, based on the interaction of the pure components as models and their properties, is described through a number of thermodynamic equations.

3.1. Evaluation of equilibrium systems

It is common to use temperature, density, and energy to determine how long structures or systems take to

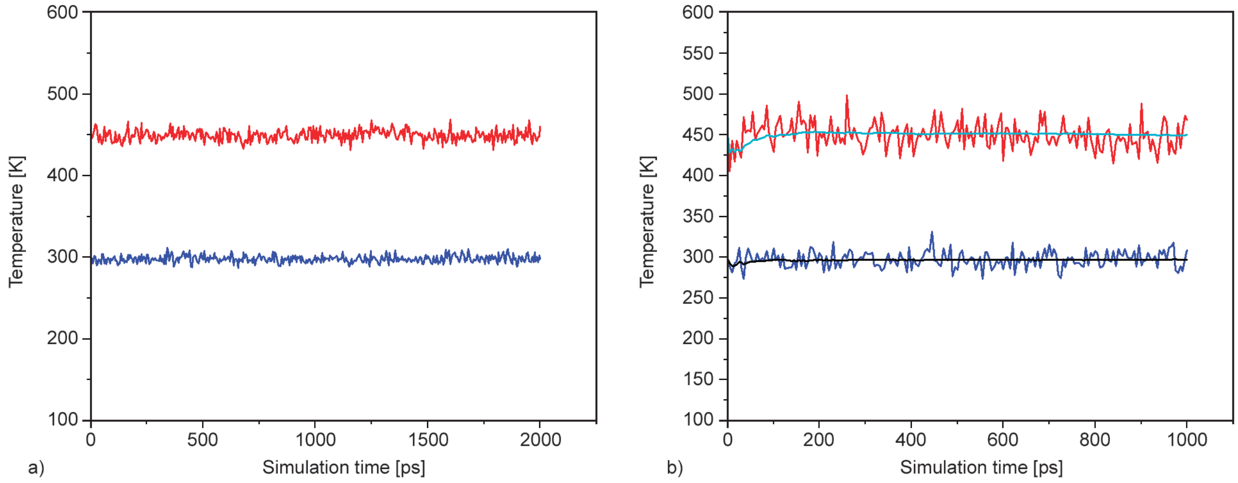

Figure 1. Temperature versus simulation time of a) LLDPE and b) wax done at 298 K (blue) and 450 K (red).

reach equilibrium in MD simulations [20, 48]. The temperature of the neat LLPDE fluctuated between 5 and 10% throughout the entire simulation (Figure 1a). This fluctuation indicates that the system was already at equilibrium when the MD simulations started. However, it took at least 200 ps for the wax structure to reach equilibrium at 298 K (Figure 1b). The wax model behaved like a hot liquid or solution at 450 K because the temperature deviated more than 25% from the average.

Density instead of volume is sometimes used to investigate the glass transition of many polymers, and the density values obtained from the NPT simulations were determined from equilibrated LLDPE models [49, 50]. The density of the neat LLPDE reached a constant value after only 250 ps (Figure 2a). At the same time, the wax density equilibrated after 200 ps (Figure 2b). These values are very similar to the experimental values and densities used for the simulations by Choi [18] (Table 1). The equilibrium structures of both LLDPE and wax were further used to determine the solubility parameters applied in calculating the Flory-Huggins parameter.

For the 60/40 w/w LLPDE/wax blend, the temperature fluctuated between 5 and 10% after 100 ps (Figure 3) at 298 and 450 K, indicating that the system reached equilibrium very quickly. The density ramped up from 0.6 g·cm^{-1} to stable equilibrium values of 0.837 g·cm^{-3} at 298 K and 0.739 g·cm^{-3} at 450 K during the first 100 ps of the simulation, and these values are in line with those obtained by other researchers [18, 51]. The blend density stabilised at these values after 200 ps (Figure 4). Density is used to investigate the glass transition of many binary systems for miscibility studies [52–54]. The time evolution density profiles during NPT-MD simulations have been used to assess the equilibration of the blends before the systems were used for further simulations of properties [34, 38]. Therefore, the density evolution of the LLDPE/wax blends was stable for 500 ps, so when the simulation time was over 2000 ps, no changes in the density evolution were observed.

Energy versus temperature was successfully used in a previous study to investigate the interaction of polyethylene molecules of varying chain lengths [19]. Figure 5 shows the potential energy, van der Waals

Table 1. Densities of the model systems of polyethylene used by Choi [18].

Temperature [K]	425	450	475	500	525
Density [g·cm^{-3}]	0.779	0.766	0.753	0.740	0.725

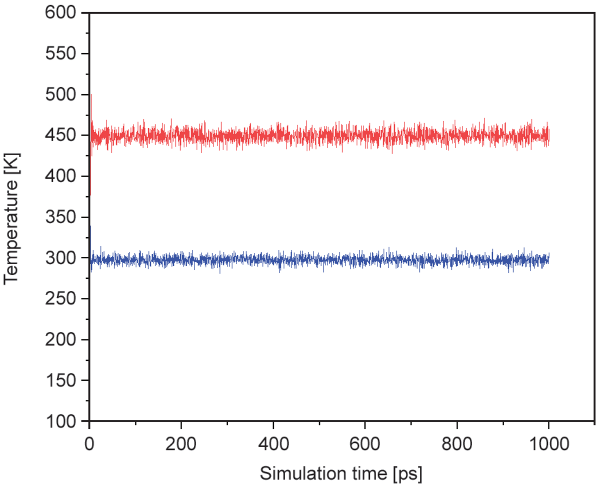

Figure 3. Temperature versus simulation time of 60/40 w/w LLDPE/wax – simulations done at 298 K (blue) and 450 K (red).

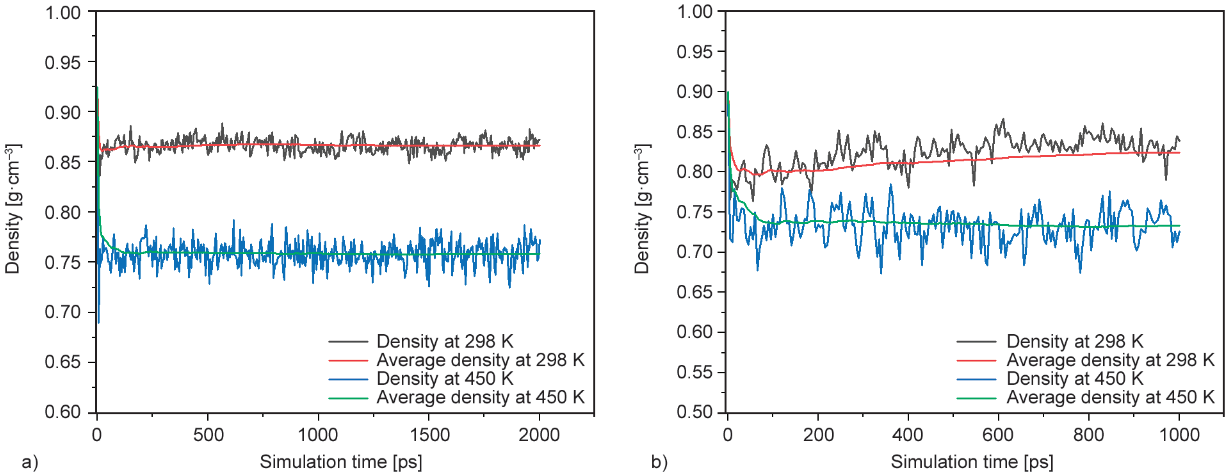

Figure 2. a) Density of LLDPE *versus* simulation time at 298 K (black) and 450 K (blue); b) density of the equilibrating wax (5 chains in a box) against simulation time at 298 K (black) and 450 K (blue).

energy, and kinetic energy for the neat LLDPE and wax. The systems' potential and van der Waals energies are responsible for long-range interactions. The movement of atoms and chains generates the kinetic energy during the simulation. The models of both neat wax and neat LLDPE reached equilibrium within 500 ps.

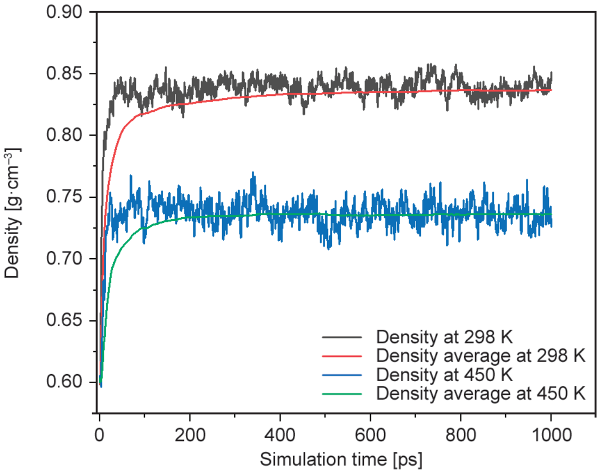

Figure 4. Density *versus* simulation time of 60/40 w/w LLDPE/wax – simulations done at 298 K (black) and 450 K (blue).

Similarly, the MD simulations that were conducted on the other LLDPE/wax systems: 95/5, 90/10, 80/20, and 70/30 w/w (graphs not presented here), reached equilibrium within the first 1000 ps of simulation time. Therefore, after completing all the MD simulations for blends (amorphous cells) shown in Figure 5, the densities of equilibrium structures were obtained at 298 K (solid-state) and 450 K (molten-state). The different energies (kinetic, potential, and van der Waals) of the same system (Figures 6 and 7) fluctuate between 5 to 10% after 100 ps. This fluctuation indicates that the system has reached equilibrium because the standard deviation of the total energy was only 3.2%. The systems that contained different polymer chains interacting with each other in the unit cell took 100 ps simulation time to get to equilibrium.

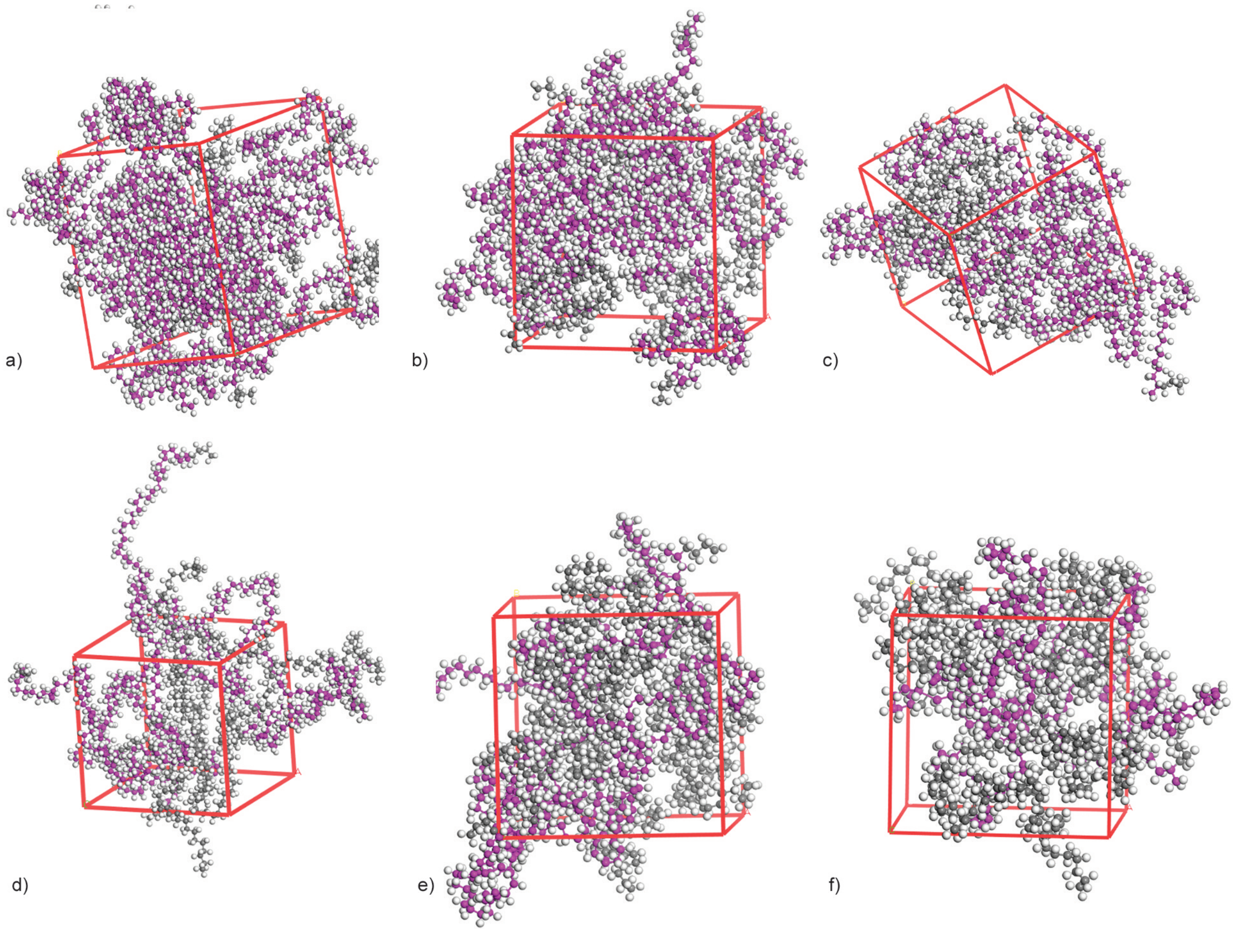

Figure 5. The amorphous cells of the short LLDPE/wax blends from MD simulations: a) 95/5 w/w LLDPE/wax; b) 90/10 w/w LLDPE/wax; c) 80/20 w/w LLDPE/wax; d) 70/30 w/w LLDPE/wax, e) 60/40 w/w LLDPE/wax; f) 50/50 w/w LLDPE/ wax (LLDPE – the purple atoms represent the backbone carbons, the grey atoms the carbon branches, and the white atoms the hydrogens; wax – the carbons are represented by grey atoms and the hydrogens by white atoms [33]).

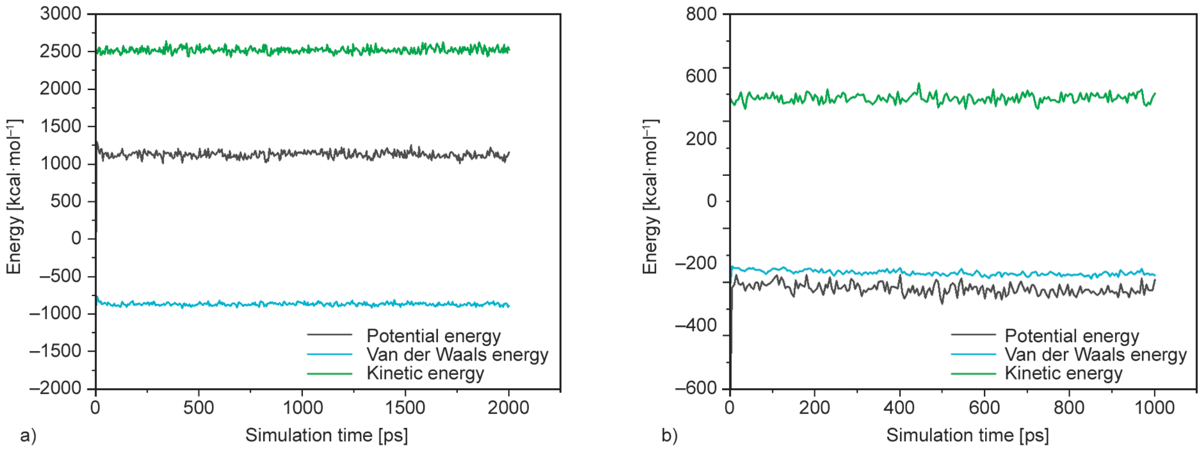

Figure 6. a) Different energies of LLDPE as a function of MD simulation time at 298 K; b) energies of wax equilibrating at 298 K.

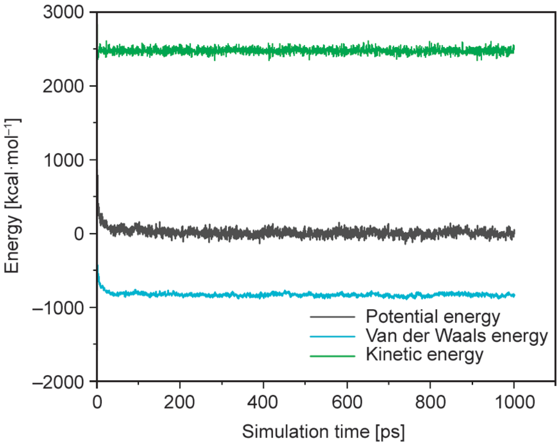

Figure 7. Different energies of 60/40 w/w LLDPE/wax as a function of MD simulation time at 298 K.

Chains with 520 carbons in the backbone and 70 branches for each chain were used to create the blends to study the miscibility of LLDPE and wax. The equilibrium structures of the LLDPE/wax blends with four different mass ratios (95/5, 90/10, 80/20, and 70/30 w/w) were obtained at 298 K (solid-state) and 450 K (molten state) using MD. The densities of all the blends reached equilibrium after 200 ps. The generated blends of various mass ratios equilibrated well using NPT dynamics. Enough simulation time was therefore applied to all the systems to study the miscibility of the LLDPE/wax blends. All the blends were produced from LLDPE-70 and C36 wax for the MD simulations. This approach was further based on the fact that the number of branches had no observable effect on the solubility parameter in method development and validation of the models.

3.2. Miscibility analysis of the blends

Polymer miscibility is defined as the ability of two or more polymers to form a single-phase mixture at a particular temperature, pressure, and composition. The miscibility of two polymers depends on specific interactions between the polymer chains. The entropy factor explains this in Equation (7), which represents the second law of thermodynamics. The change in free energy, ΔG, of a reaction is given in Equation (7). If ΔG is positive, the reaction is non-spontaneous, and if ΔG is negative, it is spontaneous:

$$\Delta G_\mathrm{M} = \Delta H_\mathrm{M} - T\Delta S_\mathrm{M} \qquad (7)$$

where ΔH_M is the mixing enthalpy, T is the temperature, and ΔS_M is the mixing entropy.

The miscibility of the blends is usually controlled by four factors: chemical structure, crystallinity, molar mass distribution, and molecular architecture of the individual polymers. The miscibility of polymer blends has been theoretically and experimentally investigated through several methods. Atomistic MD has been successfully used to investigate the miscibility of many polymer blend systems. Several authors [23, 27, 55] have used a combination of theoretical equations to model the miscibility in molecular dynamics, such as the Flory-Huggins theory, glass transition temperature, and pair correlation functions. These methods describe miscibility in terms of the degree of dispersion, phase morphology, or degree of interaction between the components. The nature of the chemical structures of both wax and polyethylene, in particular, LLDPE with a degree of branch content and distribution, is complex in a blend. It was, therefore, imperative to use methods used by other researchers to investigate the miscibility of LLDPE/wax blends. The results obtained from all these methods are discussed below.

Flory-Huggins theory

The Flory-Huggins theory is based on the mathematical equation (Equation (8)) that describes the thermodynamics of polymer-polymer mixtures. It considers the dissimilarity of molecules by adapting the entropy of mixing:

$$\Delta G_\mathrm{m} = RT\left[\chi\phi_1\phi_2 + \frac{\phi_1}{N_1}\ln\phi_1 + \frac{\phi_2}{N_2}\ln\phi_2\right] \tag{8}$$

where G_m is the Gibbs energy of mixing, R is the gas constant, T is the temperature, χ the Flory-Huggins interaction parameter, ϕ the volume fraction, N the chain length of the polymer, while 1 and 2 denote the components in the blend.

The Flory-Huggins theory describes polymer interactions in blends through their solubility and interaction parameters. Atomistic MD is often used to determine the solubility of the blends using amorphous cells or directly the solubility of pure components. The solubility of the pure components and the blends are then used in a set of equations to calculate the interaction parameters of the various binary blend systems. The polymer miscibility relationships are then established. The parameters are briefly described below. It is important to note that Equation (8) requires an additional term to account for negative free energy when the polymer-polymer interaction parameter is affected by the presence of favourable intermolecular interactions; most commonly, non-random hydrogen bonds [56]. Equation (8) has therefore been mostly applied to solvent-solvent and polymer-solvent mixtures because the combinatorial entropy of mixing is finite and contributes to the free energy of mixing.

Hildebrand solubility parameter (δ)

The Hildebrand solubility parameter (Equation (9)), by definition, measures the solubility of a polymer in a solvent and estimates the degree of interaction between the polymer and solvent. It is an important physical quantity used to determine the miscibility of materials and is defined in terms of cohesive energy density (CED). Thermodynamically, materials with similar solubility parameters are compatible [57, 58]. Solubility is used to thermodynamically determine the Flory-Huggins interaction parameter (χ). The interaction parameter describes the strength of pair(s) of polymer-polymer interactions and controls the degree of miscibility for a specific pair and/or their compatible ratios at a given temperature [59]. The solubility parameter is related to the cohesive energy density (CED) of the molecules (Equation (9)):

$$\delta = \sqrt{CED} \equiv \sqrt{\frac{E_\mathrm{coh}}{V}} \tag{9}$$

where E_coh is the cohesive energy per mol and V is the molar volume. E_coh/V is, therefore, the cohesive energy density. The interaction parameter (χ) is given by Equations (10) or (11):

$$\chi_\mathrm{wLL} = \frac{V_\mathrm{m}(\delta_\mathrm{w} - \delta_\mathrm{LL})^2}{RT} \tag{10}$$

$$\chi_\mathrm{wLL} = \frac{\Delta E_{mix}}{RT\phi_\mathrm{w}\phi_\mathrm{LL}}V_\mathrm{m} \tag{11}$$

where V_m is the monomer (repeat) unit volume per mol, R is the gas constant, and T is temperature. ΔE_mix is the energy change of mixing and ϕ_w and ϕ_LL are the volume fractions of wax and LLDPE. The critical interaction value is calculated through Equation (12) [56, 60], with the assumption that the densities of the two polymers are equal to 1.0 g·cm^{-3}:

$$\chi_\mathrm{c} = (\chi_\mathrm{wLL})_\mathrm{critical} = \frac{1}{2}\left(\frac{1}{\sqrt{m_\mathrm{w}}} + \frac{1}{\sqrt{m_\mathrm{LL}}}\right)^2 \tag{12}$$

Positive interaction parameter values commonly mean immiscibility for high molecular weight polymers. However, it is necessary to compute the critical value of the interaction parameter (Equation (12)), where m_LL and m_w represent the degree of polymerization or number of monomers (number of repeat units) of the pure components, in this case, LLDPE and wax, used to generate the blends. The calculated value of χ_c equals 0.050 based on an m_LL of 200 from the LLDPE molecular structure used to do atomics dynamics and an m_w of 18 for the wax chain. The blends would be miscible if $(\chi_\mathrm{wLL})_\mathrm{critical}$ is larger than χ_wLL.

The first energy of mixing is determined through Equation (13). This equation defines the energy of mixing in a binary mixture of polymer blends:

$$\Delta E_\mathrm{mix} = \phi_\mathrm{w}\left(\frac{E_\mathrm{coh}}{V}\right)_\mathrm{w} + \phi_\mathrm{LL}\left(\frac{E_\mathrm{coh}}{V}\right)_\mathrm{LL} - \left(\frac{E_\mathrm{coh}}{V}\right)_\mathrm{mix} \tag{13}$$

where ΔE_mix is the energy change of mixing per unit volume, ϕ_w and ϕ_LL are the volume fractions of wax and LLDPE, $\phi_\mathrm{w} + \phi_\mathrm{LL} = 1$. The word 'mix' denotes the cohesive energy density of the mixture (blend). The symbols outside the parentheses denote the mole fraction of each pure component involved in preparing the polymer blend, while the values within the brackets refer to the cohesive energy densities (E_{coh}/V) of the individual polymers and the binary blend.

The solubility parameter of LLDPE was found to be between 2 and 4 $\text{MPa}^{0.5}$ (Table 2), smaller than that of wax (for both 1 and 5 chains per unit cell). If the difference in solubility parameter between two interacting polymers is less than 2 $\text{MPa}^{0.5}$ [20], the polymers are expected to be miscible [20, 61], and for polymer-drug interactions, the solubility parameter difference for miscible systems was found to reach a limit of 7 $\text{MPa}^{0.5}$ [62]. This difference in the solubility parameter limit worked when the polymer-polymer interactions in question were of equal molecular weight [56]. For the Flory-Huggins interaction parameter (χ) of polymers with strong specific interaction, such as hydrogen bonding, the solubility parameter difference was found to be more than 5 $\text{MPa}^{0.5}$ [63]. The difference in solubility parameter limit may therefore differ based on the type of polymer-polymer interactions. According to the difference in solubility parameters, partial to total miscibility is expected in LLDE/wax blends because the difference in solubility parameters between these components is below 4 and over 2 $\text{MPa}^{0.5}$ (Table 2). It is commonly accepted that the solubility of two materials is only possible when their intermolecular attractive forces are similar, therefore, polymers with similar solubility parameter values are expected to be miscible. Wax is also a good plasticizer which acts as a solvent in the amorphous regions of the semi-crystalline LLDPE, creating a relative degree of miscibility that is composition dependent. Therefore, even though the solubility parameter difference is over 2 $\text{MPa}^{0.5}$, the wax acting as a solvent surpasses that limitation. If the van der Waals or other interacting forces between polymer molecules are very small, there is no good interaction, and the blends would be immiscible.

There are no hydrogen bonding interactions between LLDPE and wax, therefore, the theory discussed here is sufficiently applicable to the systems tested. However, the interactions of wax and LLDPE provides a unique structural situation to investigate miscibility. First of all, the chain length of wax must be limited to model the actual soft paraffin wax used in the experiments [33]. Therefore, the special case of looking at the effect of the degree of polymerization on the critical interaction parameter [56] would not apply to the LLDPE/wax systems where there is a large difference in molecular weights. In fact, it is better to look at wax and LLDPE interactions based on the polymer-solvent interaction theory [60]. Experimentally it has been established that branch content controls the miscibility of LLDPE with other polyethylenes [64], and therefore wax is expected to show similar interactions.

The interaction parameters for all the blends investigated in this study, especially at 298 K, are lower than the critical interaction parameter (Figure 8). Many computational polymer scientists say that if the Flory-Huggins interaction parameters are smaller than the critical interaction parameter, it means that the investigated system is miscible; if slightly larger, then partial miscibility would sometimes be possible; otherwise, the binary blends would be immiscible [23–25, 28, 32]. However, the accuracy of the calculated solubility parameter, to some extent, affects the conclusions drawn from such miscibility studies. According to the interaction parameters calculated for all the compositions, the modelled binary blends between wax and LLDPE are miscible. There is no reason to doubt the accuracy of the simulations in the investigated systems because of the level of the

Table 2. Simulation results of the modelled LLDPE/wax blends.

Number of chains per cell	Composition [wt% LLDPE]	The density of the system [g·cm^{-3}]		Solubility parameter [$\text{MPa}^{0.5}$]		χ_{AB} [–]	
		298 K	450 K	298 K	450 K	298 K	450 K
1 LLDPE	100	0.863	0.763	11.0	9.5	N/A	N/A
1 wax	0	0.848	0.801	15.8	15.9	N/A	N/A
5 wax	0	0.842	0.732	14.3	14.6	N/A	N/A
1 LLDPE, 1 wax	95	0.857	0.753	11.2	9.6	–2.77	0.61
1 LLDPE, 2 wax	90	0.854	0.748	12.7	10.9	–2.51	–1.18
1 LLDPE, 4 wax	80	0.852	0.751	12.9	11.2	–0.43	–0.13
2 LLDPE, 15 wax	70	0.842	0.741	14.3	12.1	–3.21	–2.61
1 LLDPE, 12 wax	60	0.837	0.736	15.1	12.5	–0.05	–0.50

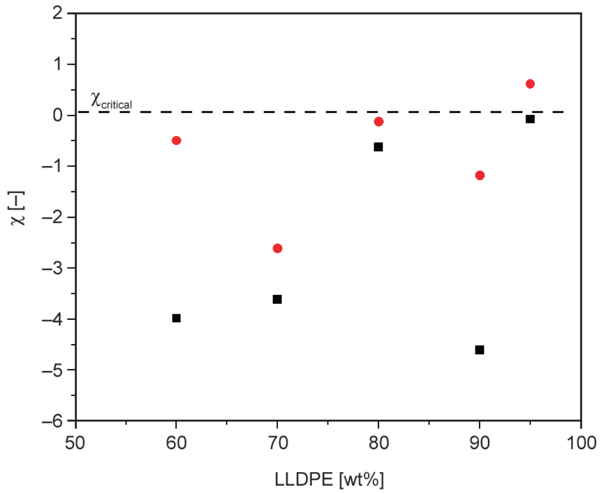

Figure 8. Interaction parameters for the LLDPE/wax blends determined at 298 K (black squares) and 450 K (red circles).

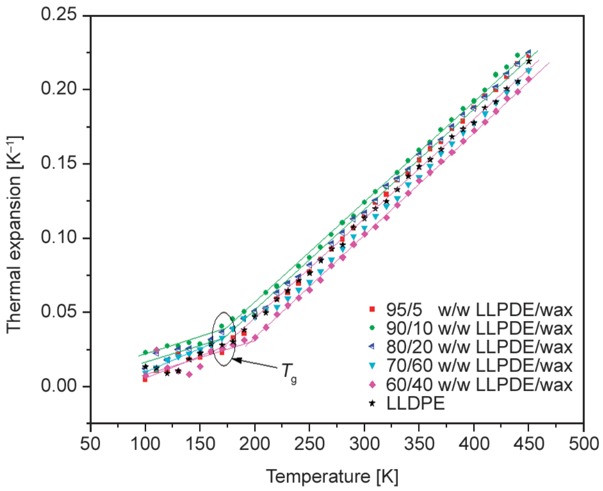

Figure 9. Thermal expansion versus temperature for the LLDPE/wax blends.

systems' equilibrations shown in Section 3.1. This conclusion is, however, contradictory to the experimental results discussed in our previously published article [33]. Experimentally, up to 5 wt.% wax in the blend was completely miscible with the LLDPE. At higher wax contents, partial miscibility was observed. An explanation for this apparent difference between the simulation and experimental results will be given later in the discussion.

Glass transition

Volume thermal expansion is defined by the change in size or volume of an object undergoing thermal expansion due to a temperature change. The concept of free volume, the space in the polymer liquid or solid sample not occupied by molecules, is commonly related to the glass transition temperature. Therefore, as the temperature of the molten polymer blend is slowly decreased, the free volume between the molecules is reduced until there is little free space to allow molecular movement. The polymer changes from a rubbery state to a 'frozen' glassy state and the temperature at which the change occurs is called the glass transition temperature [65].

Figure 9 shows the thermal expansion obtained from MD simulations (simulating a slow cooling process) of neat LLDPE and the blends, plotted against temperature. There is only one glass transition temperature (circled) at 175 K for neat LLDPE and all the blends, except for a shift to 200 K observable for the 60/40 w/w LLDPE/wax blend. One glass transition temperature of a binary blend indicates a miscible, continuous phase morphology if the two components in the blend if both have glass transitions and if the glass transitions occur at different temperatures. The results from the thermal expansion theoretically agree with the Flory-Huggins interaction parameter, as determined by the solubility parameter. However, since wax is almost 100% crystalline and does not show a glass transition, the above cannot be applied to the system under investigation. Therefore, a single glass transition cannot be used as complementary evidence of complete miscibility between LLDPE and wax.

3.3. Interaction of polymer chains based on the pair correlation function

The pair correlation function also called the radial distribution function ($g_{AB}(r)$), describes how the density of electrons or atoms varies as a function of the distance from a reference point (Equation (14)). It is the probability of finding a particle's centre at a distance from the centre of another particle. The function can be applied in inter-and intra-chain interactions in polymer blends.

$$g_{AB}(r) = \frac{1}{\rho_{AB}4\pi r^2\delta_r}\frac{\sum_{t=1}^{K}\sum_{j=1}^{N_{AB}} N_{AB}(r \to r+\delta_r)}{N_{AB}\cdot k} \tag{14}$$

The function is mostly used to characterise the structure of the molecules. N_{AB} is the total number of atoms of A and B in the system, δ_r is the average number of atom pairs between r and $r + \delta_r$, and ρ_{AB} is the bulk density [29].

Intra-molecular pairs ($g_{intra}(r)$) of carbon atoms of pure LLDPE, wax, and their blends are shown in Figure 10. The highest at 1.2 Å shows bond connectivity of

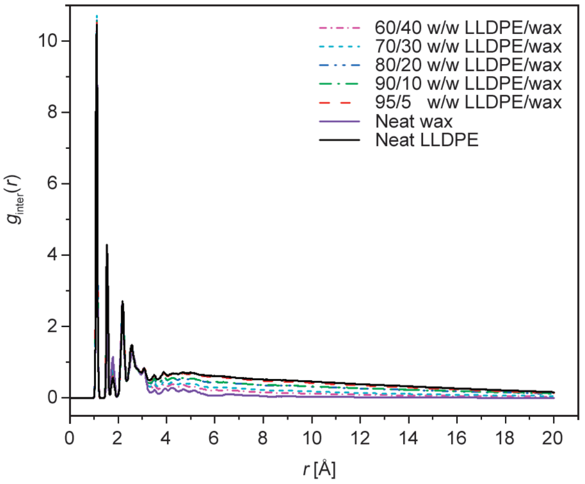

Figure 10. The radial distribution function of the intramolecular interactions of like pairs and unlike pairs in 60/40 w/w LLDPE/wax.

either LLDPE, wax, or any of the blends. The next four peaks are at atomic pairs without connectivity with the spatial vicinities in the following order of numbers: 1.5, 1.75, 2.25, 2.5, and 3 Å. Because the wax and LLDPE have very similar structures, there are no significant changes in the intramolecular interactions with increased wax content in the blends. However, the curves of the blends overlap for both the wax and LLDPE structures.

Figure 11 shows the interchain pair ($g_{inter}(r)$) correlation between the LLDPE and wax atoms. The long LLDPE chains were simulated in Figure 11a. There was an increase in the ($g_{inter}(r)$) value with the addition of more wax into the blends. A very similar trend was observed for the modulus of the blends in the DMA experiments [33]. In the article, the higher moduli were attributed to more wax crystals in the amorphous phase of LLDPE, and these crystals acted as physical cross-links between the LLDPE chains. This observation explains the increasing value of ($g_{inter}(r)$) with increasing wax content. The long chains of LLDPE are, therefore, semi-miscible with the wax in the blends at all the blend ratios. However, with short LLDPE chains (Figure 11b), there is almost no difference between the chain interactions in the blends when compared to those of either wax or LLDPE. It, therefore, looks as if the miscibility between the wax and LLDPE probably depends upon chain length. This observation explains the complete miscibility at low wax contents in the blends and the partial miscibility at higher wax contents. The wax would preferably co-crystallise with the short LLDPE chains. When the wax content was relatively high, only some of the wax chains could co-crystallise with the smaller number of short LLDPE chains, while the remainder of the wax chains crystallised separately in the amorphous phase of the LLDPE. Other researchers also found that miscibility was affected by either length or self-concentration due to the chain connectivity of the polymers when MD simulations were applied to the models [21, 28].

3.4. Dissipative particle dynamics (DPD) of LLDPE/wax blends

The DPD simulation results of long chains of LLDPE/wax blends are shown in Figure 12. These simulations were used to investigate the effect of wax content on the morphology of LLDPE/wax binary systems. Miscibility or separate wax crystallisation is not clear in Figures 12b and 12c. However, Figure 12a clearly shows the complete miscibility of the wax and the LLDPE. In contrast, Figures 12d,

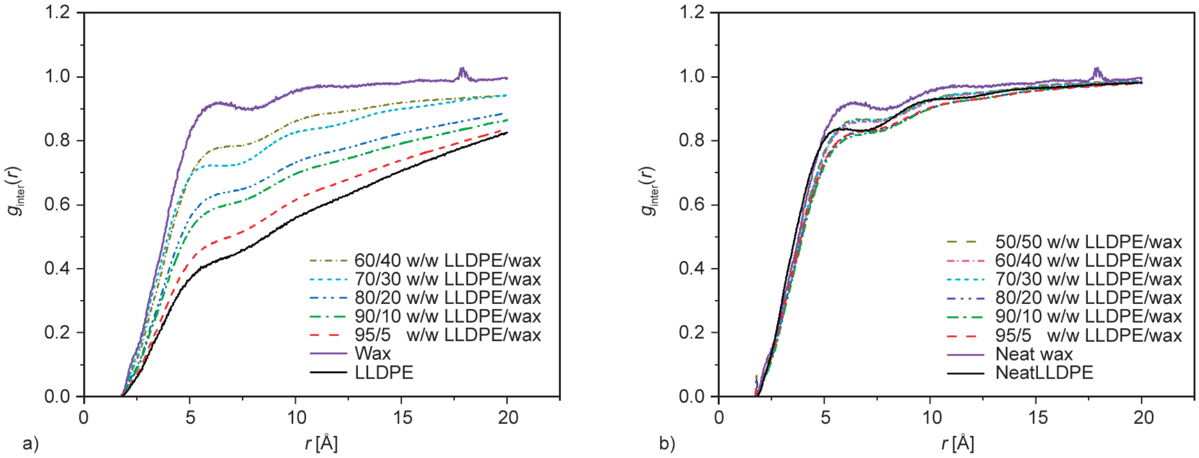

Figure 11. The radial distribution function of the intermolecular interactions of like pairs and unlike pairs in LLDPE/wax blends: a) long LLDPE chains at 450 K; b) short LLDPE chains at 450 K.

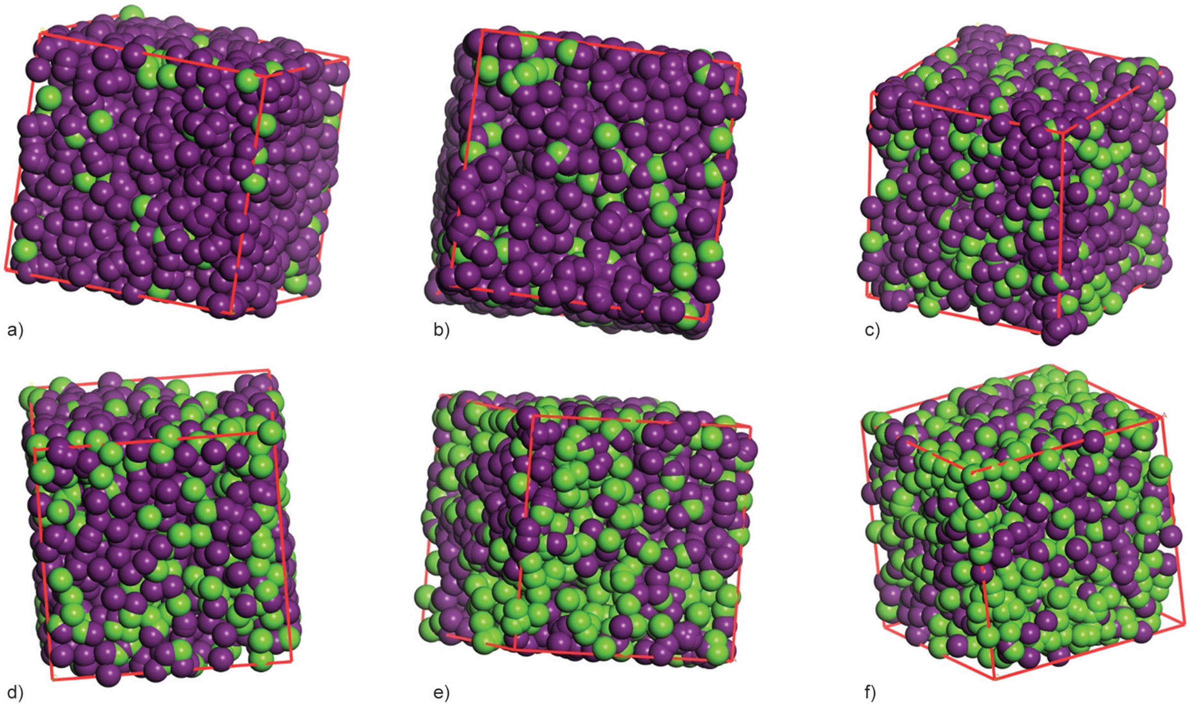

Figure 12. Morphologies of LLDPE/wax blends from DPD simulations (LLDPE: purple; wax: green): a) 95/5 w/w LLDPE/wax; b) 90/10 w/w LLDPE/wax; c) 80/20 w/w LLDPE/wax; d) 70/30 w/w LLDPE/wax, e) 60/40 w/w LLDPE/wax; f) 50/50 w/w LLDPE/wax.

12e, and 12f show separate entities in the blend that contain only wax chains, which is in line with the observation in the results of our previously published work [33] that the blends with higher wax content showed partial miscibility. The miscibility difference observed between the models and experiments could be the result of the high branch content used in the models compared to the 2.3% branch content for the LLDPE used to prepare the blends in the experiments [33]. Therefore, models of low branch content should be used to compare the miscibility of the LLDPE/wax models with that from the actual experiments. It would be interesting to do DPD simulations whereby both chain length and branch content of LLDPE are varied as a function of the same wax chain lengths.

Table 3 shows the Flory-Huggins values calculated using the solubility parameters of wax and LLDPE. The repulsion interaction values used as input to do the DPD simulations to get the morphologies of Figure 12 are also in the same table.

Table 3. Flory-Huggins interaction parameters and repulsion parameters, obtained using solubility parameters calculated in Synthia, from the DPD calculations.

Interacting polymers	Flory-Huggins parameter		Repulsion parameters for DPD	
	LLDPE-70	Wax (C36)	LLDPE-70	Wax (C36)
LLDPE-70	0	0.152	25	37
Wax (C36)	0.152	0	37	25

4. Conclusions

MD studies were used to investigate the miscibility of LLDPE/wax at mass ratios similar to those used in the experiments. The solubility parameter of the pure components and blends was computed to determine the interaction parameter of all the binary systems. Because the $(\chi_{AB})_{critical}$ value was larger than χ_{AB} for all the investigated ratios, it was concluded that, based on these results alone, the wax was miscible with LLDPE. The results from the Flory-Huggins theory could not be supported by the single T_g values obtained for the blends since wax is almost 100% crystalline and does not show a glass transition. However, the simulations showed a difference in the interaction of wax chains with respectively short- and long LLDPE chains. This observation explained the complete miscibility of LLDPE/wax blends with low wax contents and the partial miscibility when the wax contents were so high that there were not enough short LLDPE chains that could co-crystallise with all the wax chains. Both complete and partial miscibility of the blends was further visible in the DPD simulations. The interactions of wax and

LLDPE provides a unique structural situation to investigate miscibility compared to most homopolymer miscibility studies done using simulations. The chain length of wax must be carefully chosen to model the actual soft paraffin wax used in the experiments. The interaction of wax with LLDPE is also dependent on the branch content, and changes in miscibility of the LLDPE/wax blends based on branches is possible. Therefore, the chain length of wax and number of branches of the LLDPE models used in this work is purely based on the simulations studies which were complemented by the experiments [2].

Acknowledgements

The University of the Free State is acknowledged for financial support through the Postgraduate School, and for providing the computer hardware resources. The Centre for High Performance Computing, and North-West University – High Performance Computing, are acknowledged for providing all the software resources used in the project.

References

[1] Lee C. H., Choi H. K.: Crystalline morphology in high-density polyethylene/paraffin blend for thermal energy storage. Polymer Composites, **19**, 704–708 (1998). https://doi.org/10.1002/pc.10143

[2] Gabriel C., Kaschta J., Münstedt H.: Influence of molecular structure on rheological properties of polyethylenes. Rheological Acta, **37**, 7–20 (1998). https://doi.org/10.1007/s003970050086

[3] Luyt A. S., Geethamma V. G.: Effect of oxidized paraffin wax on the thermal and mechanical properties of linear low-density polyethylene-layered silicate nanocomposites. Polymer Testing, **26**, 461–470 (2007). https://doi.org/10.1016/j.polymertesting.2006.12.015

[4] Hasnain S. M.: Review on sustainable thermal energy storage technologies, Part I: Heat storage materials and techniques. Energy Conversion and Management, **39**, 1127–1138 (1998). https://doi.org/10.1016/S0196-8904(98)00025-9

[5] Chen F., Wolcott M. P.: Miscibility studies of paraffin/polyethylene blends as form-stable phase change materials. European Polymer Journal, **52**, 44–52 (2014). https://doi.org/10.1016/j.eurpolymj.2013.09.027

[6] Lohse D. J., Graessley W. W.: Thermodynamics of polyolefin blends. in 'Polymer blends' (eds.: Paul D. R., Bucknall C. B.) Wiley, New York, Vol. 1, 219–238 (1999).

[7] Cai Y., Wei Q., Huang F., Lin S., Chen F., Gao W.: Thermal stability, latent heat and flame retardant properties of the thermal energy storage phase change materials based on paraffin/high density polyethylene composites. Renewable Energy, **34**, 2117–2123 (2009). https://doi.org/10.1016/j.renene.2009.01.017

[8] Krupa I., Miková G., Luyt A. S.: Phase change materials based on low-density polyethylene/paraffin wax blends. European Polymer Journal, **43**, 4695–4705 (2007). https://doi.org/10.1016/j.eurpolymj.2007.08.022

[9] Hato M. J., Luyt A. S.: Thermal fractionation and properties of different polyethylene/wax blends. Journal of Applied Polymer Science, **104**, 2225–2236 (2007). https://doi.org/10.1002/app.25494

[10] Molefi J. A., Luyt A. S., Krupa I.: Comparison of LDPE, LLDPE and HDPE as matrices for phase change materials based on a soft Fischer–Tropsch paraffin wax. Thermochimica Acta, **500**, 88–92 (2010). https://doi.org/10.1016/j.tca.2010.01.002

[11] Utracki L. A.: Commercial polymer blends. Chapman and Hall, London (1998).

[12] Yang H.: Molecular dynamics simulation studies of binary blend miscibility. in 'Functional polymer blends: Synthesis, properties and performances' (ed.: Mittal V.) CRC Press, Boca Ratron, 177–192 (2012).

[13] Krupa I., Luyt A. S.: Thermal properties of uncross-linked and cross-linked LLDPE/wax blends. Polymer Degradation and Stability, **70**, 111–117 (2000). https://doi.org/10.1016/S0141-3910(00)00097-5

[14] Krupa I., Luyt A. S.: Thermal and mechanical properties of extruded LLDPE/wax blends. Polymer Degradation and Stability, **73**, 157–161 (2001). https://doi.org/10.1016/S0141-3910(01)00082-9

[15] Hill M. J., Barham P. J.: Interpretation of phase behaviour of blends containing linear low-density polyethylenes using a ternary phase diagram. Polymer, **35**, 1802–1808 (1994). https://doi.org/10.1016/0032-3861(94)90968-7

[16] Agamalian M., Alamo R. G., Kim M. H., Londono J. D., Mandelkern L., Wignall G. D.: Phase behavior of blends of linear and branched polyethylenes on micron length scales *via* ultra-small-angle neutron scattering. Macromolecules, **32**, 3093–3096 (1999). https://doi.org/10.1021/ma981091b

[17] Hill M. J., Morgan R. L., Barham P. J.: Minimum branch content for detection of liquid-liquid phase separation, using indirect techniques, in blends of polyethylene with ethylene-octene and ethylene-butene copolymers. Polymer, **38**, 3003–3009 (1997). https://doi.org/10.1016/S0032-3861(96)00871-3

[18] Choi P.: Molecular dynamics studies of the thermodynamics of HDPE/butene-based LLDPE blends. Polymer, **41**, 8741–8747 (2000). https://doi.org/10.1016/S0032-3861(00)00279-2

[19] Wang J., Zhu X., Lu X., Zhou Z., Wang G.: On structures and properties of polyethylene during heating and cooling processes based on molecular dynamics simulations. Computational and Theoretical Chemistry, **1052**, 26–34 (2015). https://doi.org/10.1016/j.comptc.2014.11.015

[20] Wei Q., Wang Y., Che Y., Yang M., Li X., Zhang Y.: Molecular mechanisms in compatibility and mechanical properties of polyacrylamide/polyvinyl alcohol blends. Journal of the Mechanical Behavior of Biomedical Materials, **65**, 565–573 (2017). https://doi.org/10.1016/j.jmbbm.2016.09.011

[21] Glova A. D., Falkovich S. G., Dmitrienko D. I., Lyulin A. V., Larin S. V., Nazarychev V. M., M. Karttunen M., Lyulin S. V.: Scale-dependent miscibility of polylactide and polyhydroxybutyrate: Molecular dynamics simulations. Macromolecules, **51**, 552–563 (2018). https://doi.org/10.1021/acs.macromol.7b01640

[22] de Arenaza I. M., Hernandez-Montero N., Meaurio E., Sarasua J-R.: Competing specific interactions investigated by molecular dynamics: Analysis of poly(*p*-dioxanone)/poly(vinylphenol) blends. The Journal of Physical Chemistry B, **117**, 719–724 (2013). https://doi.org/10.1021/jp310340v

[23] Fu Y., Liao L., Lan Y., Yang L., Mei L., Liu Y., Hu S.: Molecular dynamics and mesoscopic dynamics simulations for prediction of miscibility in polypropylene/polyamide-11 blends. Journal of Molecular Structure, **1012**, 113–118 (2012). https://doi.org/10.1016/j.molstruc.2011.12.026

[24] Fu Y., Liao L., Yang L., Lan Y., Mei L., Liu Y., Hu S.: Molecular dynamics and dissipative particle dynamics simulations for prediction of miscibility in polyethylene terephthalate/polylactide blends. Molecular Simulations, **39**, 415–422 (2013). https://doi.org/10.1080/08927022.2012.738294

[25] Gai J-G., Li H-L., Schrauwen C., Hu G-H.: Dissipative particle dynamics study on the phase morphologies of the ultrahigh molecular weight polyethylene/ polypropylene/poly(ethylene glycol) blends. Polymer, **50**, 336–346 (2009). https://doi.org/10.1016/j.polymer.2008.10.020

[26] Yang H., Li Z-S., Lu Z-Y., Sun C-C.: Computer simulation studies of the miscibility of poly(3-hydroxybutyrate)-based blends. European Polymer Journal, **41**, 2956–2962 (2005). https://doi.org/10.1016/j.eurpolymj.2005.06.009

[27] Thomas S., Grohens Y., Jyotishkumar P.: Characterization of polymer blends: Miscibility, morphology and interphases. Wiley, Weinheim (2015).

[28] Lodge T. P., McLeish T. C. B.: Self-concentrations and effective glass transition temperatures in polymer blends. Macromolecules, **33**, 5278–5284 (2000). https://doi.org/10.1021/ma9921706

[29] Luo Z., Jiang J.: Molecular dynamics and dissipative particle dynamics simulations for the miscibility of poly (ethylene oxide)/poly(vinyl chloride) blends. Polymer, **51**, 291–299 (2010). https://doi.org/10.1016/j.polymer.2009.11.024

[30] de Arenaza I. M., Meaurio E., Coto B., Sarasua J-R.: Molecular dynamics modelling for the analysis and prediction of miscibility in polylactide/polyvinilphenol blends. Polymer, **51**, 4431–4438 (2010). https://doi.org/10.1016/j.polymer.2010.07.018

[31] Zhang M., Choi P., Sundararaj U.: Molecular dynamics and thermal analysis study of anomalous thermodynamic behavior of poly(ether imide)/polycarbonate blends. Polymer, **44**, 1979–1986 (2003). https://doi.org/10.1016/S0032-3861(03)00054-5

[32] Wang Y-C., Ju S-P., Cheng H-Z., Lu J-M., Wang H-H.: Modeling of polyethylene and functionalized CNT composites: A dissipative particle dynamics study. Journal of Physical Chemistry C, **114**, 3376–3384 (2010). https://doi.org/10.1021/jp909644b

[33] Mosoabisane M. F. T., Luyt A. S., van Sittert C. G. C. E.: Comparative experimental and modelling study of the thermal and thermo-mechanical properties of LLDPE/wax blends. Journal of Polymer Research, **29**, 296 (2022). https://doi.org/10.1007/s10965-022-03136-w

[34] Boomstra M. W., van Asseldonk M. W. J., Geurts B. J., Nazarychev V. M., Lyulin A.V.: Effects of branching and polydispersity on thermal conductivity of paraffin waxes. International Journal of Heat and Mass Transfer, **195**, 123192 (2022). https://doi.org/10.1016/j.ijheatmasstransfer.2022.123192

[35] Glova A. D., Volgin I. V., Nazarychev V. M., Larin S. V., Lyulin S.V., Gurtovenko A. A.: Toward realistic computer modeling of paraffin-based composite materials: Critical assessment of atomic-scale models of paraffins. RSC Advances, **9**, 33834–38847 (2019). https://doi.org/10.1039/c9ra07325f

[36] Moyassari A., Gkourmpis T., Hedenqvist M. S., Gedde U. W.: Molecular dynamics simulation of linear polyethylene blends: Effect of molar mass bimodality on topological characteristics and mechanical behavior. Polymer, **161**, 139–150 (2019). https://doi.org/10.1016/j.polymer.2018.12.012

[37] Wei Y., Zhou Z., Hao T., Nie Y.: Molecular dynamics simulation on the crystallization behavior of cyclic polyethylene affected by functionalized carbon nanotubes. Journal of Applied Polymer Science, **139**, e52481 (2022). https://doi.org/10.1002/app.52481

[38] Madhuranthakam C. M. R., Pandiyan S., Penlidis A.: Performance evaluation of nonacosan-10-ol-based polyethylene packaging material using molecular dynamics simulations. Polymers, **14**, 1779 (2022). https://doi.org/10.3390/polym14091779

[39] Burke K.: Perspective on density functional theory. Journal of Chemical Physics **136**, 150901–150909 (2012). https://doi.org/10.1063/1.4704546

[40] Lesar R.: Introduction to computational material science: Fundamental to applications. Cambridge University Press, Cambridge (2013).

[41] Perdew J. P., Burke K., Wang Y.: Generalized gradient approximation for the exchange-correlation hole of a many-electron system. Physical Review B, **54**, 16533–16539 (1996). https://doi.org/10.1103/PhysRevB.54.16533

[42] Delley B.: The conductor-like screening model for polymers and surfaces. Molecular Simulation, **32**, 117–123 (2006). https://doi.org/10.1080/08927020600589684

[43] Doran M., Choi P.: Molecular dynamics studies of the effects of branching characteristics on the crystalline structure of polyethylene. The Journal of Chemical Physics, **115**, 2827–2830 (2001). https://doi.org/10.1063/1.1386907

[44] Sun H., Ren P., Fried J. R.: The COMPASS force field: Parameterization and validation for phosphazenes. Computational and Theoretical Polymer Science, **8**, 229–246 (1998). https://doi.org/10.1016/S1089-3156(98)00042-7

[45] Theodorou D. N., Suter U. W.: Atomistic modeling of mechanical properties of polymeric glasses. Macromolecules, **19**, 139–154 (1986). https://doi.org/10.1021/ma00155a022

[46] Leimkuhler B., Noorizadeh E., Penrose O.: Comparing the efficiencies of stochastic isothermal molecular dynamics methods. Journal of Statistical Physics, **143**, 921–942 (2011). https://doi.org/10.1007/s10955-011-0210-2

[47] Groot R. D., Warren P. B.: Dissipative particle dynamics: Bridging the gap between atomistic and mesoscopic simulation. Journal of Chemical Physics, **107**, 4423–4435 (1997). https://doi.org/10.1063/1.474784

[48] Wei Q., Wang Y., Li X., Yang M., Chai W., Wang K., Yang M., Zhang Y.: Study the bonding mechanism of binders on hydroxyapatite surface and mechanical properties for 3DP fabrication bone scaffolds. Journal of the Mechanical Behavior of Biomedical Materials, **57**, 190–200 (2016). https://doi.org/10.1016/j.jmbbm.2015.12.007

[49] Mhlanga P., Hassan W. A. W., Hamerton I., Howlin B. J.: Using combined computational techniques to predict the glass transition temperatures of aromatic polybenzoxazines. PLOS one, **8**, e53367 (2013). https://doi.org/10.1371/journal.pone.0053367

[50] Rudin A., Chee K. K., Shaw J. H.: Specific volume and viscosity of polyolefin melts. Journal of Polymer Science Part C: Polymer Symposia, **30**, 415–427 (1970). https://doi.org/10.1002/polc.5070300145

[51] Kavassalis T. A., Choi P., Rudin A.: Molecular models and three-dimensional solubility parameters of nonionic surfactants. in ‘Molecular simulation and industrial applications – Methods, examples, and prospects’ (eds.: Gubbins K. E., Quirke N.) Gordon and Breach, Amsterdam, 315–329 (1996).

[52] Fan Z. J., Williams M. C., Choi P.: A molecular dynamics study of the effects of branching characteristics of LDPE on its miscibility with HDPE. Polymer, **43**, 1497–1502 (2002). https://doi.org/10.1016/S0032-3861(01)00730-3

[53] Prathab B., Subramanian V., Aminabhavi T. M.: Molecular dynamics simulations to investigate polymer–polymer and polymer–metal oxide interactions. Polymer, **48**, 409–416 (2007). https://doi.org/10.1016/j.polymer.2006.11.014

[54] Harmeton I., Howlin B. J., Pratt C. R.: Simulation of the free energy of mixing for blend components in a new family of flexible polycyanurates. Polymer, **51**, 5857–5868 (2010). https://doi.org/10.1016/j.polymer.2010.09.068

[55] Mu D., Huang X-R., Lu Z-Y., Sun C-C.: Computer simulation study on the compatibility of poly(ethylene oxide)/poly(methyl methacrylate) blends. Chemical Physics, **348**, 122–129 (2008). https://doi.org/10.1016/j.chemphys.2008.03.015

[56] Coleman M. M., Serman C. J., Bhagwagar D. E., Painter P. C.: A practical guide to polymer miscibility. Polymer, **31**, 1187–1203 (1990). https://doi.org/10.1016/0032-3861(90)90208-G

[57] Lee J. N., Park C., Whitesides G. M.: Solvent compatibility of poly(dimethylsiloxane)-based microfluidic devices. Analytical Chemistry, **75**, 6544–6554 (2003). https://doi.org/10.1021/ac0346712

[58] Huang Z., Zheng F., Chen S., Lu X., van Sittert C. G. C. E., Lu Q.: A strategy for the synthesis of cyclomatrix-polyphosphazene nanoparticles from non-aromatic monomers. RSC Advances, **6**, 75552–75561 (2016). https://doi.org/10.1039/c6ra13486f

[59] Ma X., Zheng F., van Sittert C. G. C. E., Lu Q.: Role of intrinsic factors of polyimides in glass transition temperature: An atomistic investigation. The Journal of Physical Chemistry B, **123**, 8569–8579 (2019). https://doi.org/10.1021/acs.jpcb.9b06585

[60] Lloyd L. M.: Polymer blends: A comprehensive review. München, Germany (2007).

[61] Forster A., Hempenstall J., Tucker I., Rades T.: Selection of excipients for melt extrusion with two poorly water-soluble drugs by solubility parameter calculation and thermal analysis. International Journal of Pharmaceutics, **226**, 147–161 (2001). https://doi.org/10.1016/S0378-5173(01)00801-8

[62] Greenhalgh D. J., Williams A. C., Timmins P., York P.: Solubility parameters as predictors of miscibility in solid dispersions. Journal of Pharmaceutical Sciences, **88**, 1182–1190 (1999). https://doi.org/10.1021/js9900856

[63] Meaurio E., Sanchez-Rexach E., Zuza E., Lejardi A., del Pilar Sachez-Camargo A., Sarasua J-R.: Predicting miscibility in polymer blends using the Bagley plot: Blends with poly(ethylene oxide). Polymer, **113**, 295–309 (2017). https://doi.org/10.1016/j.polymer.2017.01.041

[64] Zhao L., Choi P.: A review of the miscibility of polyethylene blends. Materials and Manufacturing Processes, **21**, 135–142 (2006). https://doi.org/10.1081/AMP-200068644

[65] Young R. J., Lovell P. A.: Introduction to polymers. Taylor and Francis, Oxfordshire (2011).